A molecular basis underpinning the T cell mediated response in HLA-DQ2.2 mediated celiac disease

Yi Tian Ting[1#], Shiva Dahal-Koirala[2,3#], Hui Shi Keshia Kim[1], Shuo-Wang Qiao[2,3], Ralf Neuman[2,3], Knut E.A. Lundin[2,3,4], Jan Petersen[1, 5], Hugh H. Reid[1, 5], Ludvig M. Sollid[2,3*] & Jamie Rossjohn[1,5,6*]

[1] Infection and Immunity Program and The Department of Biochemistry and Molecular Biology, Biomedicine Discovery Institute Monash University, Clayton, Victoria 3800, Australia.

[2] Department of Immunology, University of Oslo and Oslo University Hospital-Rikshospitalet, 0372, Oslo, Norway.

[3] K. G. Jebsen Centre for Coeliac Disease Research, University of Oslo, 0424, Oslo, Norway.

[4] Department of Gastroenterology, Oslo University Hospital-Rikshospitalet, 0372 Oslo, Norway

[5] Australian Research Council Centre of Excellence in Advanced Molecular Imaging, Monash University, Clayton, Victoria 3800, Australia.

[6] Institute of Infection and Immunity, Cardiff University School of Medicine, Heath Park, Cardiff CF14 4XN, UK.

[#]joint first authors

*joint senior & corresponding authors. l.m.sollid@medisin.uio.no
 and jamie.rossjohn@monash.edu

Running title: DQ2.2-mediated celiac disease

Abstract

The highly homologous HLA-DQ2 molecules, HLA-DQ2.5 and HLA-DQ2.2, are implicated in the pathogenesis of celiac disease (CeD) by presenting gluten peptides to CD4$^+$ T cells. However, while HLA-DQ2.5 is strongly associated with disease, HLA-DQ2.2 is not, and the molecular basis underpinning this differential disease association is unresolved. We here provide structural evidence for how the single polymorphic residue (HLA-DQ2.5-Tyr22α and HLA-DQ2.2-Phe22α) accounts for HLA-DQ2.2 additionally requiring gluten epitopes possessing a serine at the P3 position of the peptide. In marked contrast to the biased T cell receptor (TCR) usage associated with HLA-DQ2.5-mediated CeD, we demonstrate with extensive single cell sequencing that a diverse TCR repertoire enables recognition of the immunodominant HLA-DQ2.2-glut-L1 epitope. The crystal structure of two CeD patient-derived TCR in complex with HLA-DQ2.2 and DQ2.2-glut-L1 (PFSEQEQPV) revealed a docking strategy, and associated interatomic contacts, which was notably distinct from the structures of the TCR:HLA-DQ2.5:gliadin epitope complexes. Accordingly, while the molecular surfaces of the antigen-binding clefts of HLA-DQ2.5 and HLA-DQ2.2 are very similar, differences in the nature of the peptides presented translates to differences in responding T cell repertoires and the nature of engagement of the respective antigen-presenting molecules, which ultimately is associated with differing disease penetrance.

Significance statement

Celiac Disease (CeD) is an autoimmune-like disorder that is triggered by the ingestion of dietary gluten. There is a strong Human Leukocyte Antigen association with the disease, with the majority of CeD patients being HLA DQ2.5 positive. While HLA-DQ2.2 is closely related to HLA-DQ2.5, it is less of a risk factor in CeD, but our understanding behind this differential disease association remained unclear. We show that small differences in the peptide-HLA landscape causes profound differences in the responding T cell repertoire, thereby providing mechanistic insight into CeD pathogenesis.

Introduction

Celiac disease (CeD) is a heritable and chronic inflammatory disorder that is caused by a maladaptive immune response to cereal gluten proteins (1). While exhibiting features of food intolerance, the disease also has many autoimmune characteristics including highly disease specific autoantibodies targeting the enzyme transglutaminase 2 (TG2). CeD patients, but not healthy subjects, have gluten-specific CD4^{+} T cells (2). These T cells, persisting for decades in patients (3), are considered drivers of the CeD pathophysiology that includes the formation of an inflammatory lesion in the proximal small intestine and the generation of autoantibodies (4). The gluten-specific T cells are uniquely restricted by disease-associated HLA-DQ allotypes, namely HLA-DQ2.5 (*HLA-DQA1*05:01/HLA-DQB1*02:01*), HLA-DQ2.2 (*HLA-DQA1*02:01:01/HLA-DQB1*02:01*) and HLA-DQ8 (*HLA-DQA1*03:01/HLA-DQB1*03:02*) (5-7). About 90% of patients affected by CeD are HLA-DQ2.5 positive, and those who do not carry HLA-DQ2.5 are equally often either HLA-DQ2.2 or HLA-DQ8. Interestingly, while the risk of the three disease-associated HLA-DQ allotypes are very different, the clinical presentations of patients with the different HLA-DQ allotypes are the same (7). This suggests that the differential risks relate to likelihood of generating an anti-gluten T cell response and once the gluten-specific T cells are established and clonally expanded, exposure to gluten leads to the same pathophysiological reactions.

The gluten peptides recognized by T cells of CeD patients are post-translationally modified. TG2 is essential in this process as the enzyme can convert glutamine residues in polypeptides to glutamate, mostly following a QXP recognition motif (8,9). Gluten proteins are exceptionally rich in such sequence motifs but naturally sparse in negatively charged residues that is required for a high affinity binding to peptide binding pockets within the antigen binding cleft of the disease associated HLA-DQ allotypes (7). The TG2-mediated deamidation of gluten peptides leads to an increase in binding affinity and the formation of kinetically stable peptide-HLA-DQ complexes (10). Hence this post-translational modification is essential for the immunogenicity of these antigens (11-13), and the immune reactions inflicting damage that ensue T cell recognition of HLA-DQ gluten peptide complexes is likely the mechanism behind the absolute association of certain HLA-DQ allomorphs with CeD (7). Generally, T cell clones restricted by the three CeD-associated HLA allotypes recognize distinct and separate sets of gluten epitopes (4,14,15). This selectivity is based on the capacity of peptides to form kinetically stable peptide HLA-DQ complexes as only peptides that form stable peptide complexes can elicit T cell clonal expansions *in vivo* (14,16).

While HLA-DQ8 binds and presents gluten peptides with glutamate at anchor positions P1 and/or P9 (15,17,18), HLA-DQ2.5 and HLA-DQ2.2 binds and presents gluten peptides with glutamate residues at anchor positions P4, P6 or P7 (15,19-23). Three known HLA-DQ2.2 restricted epitopes, namely DQ2.2-glut-L1 (PFSEQEQPV), DQ2.2-glia-α1 (QGSVQPQQL) and DQ2.2-glia-α2 (QYSQPEQPI), have sequences similar to HLA-DQ2.5 binding peptides, with the exception that they all carry serine at P3 (14,24,25). As seen for HLA-DQ2.5-restricted epitopes, the HLA-DQ2.2-restricted epitopes display a hierarchy with DQ2.2-glut-L1 being the epitope recognized by most T cells (24). In binding experiments with DQ2.2-glut-L1 variant peptides substituted at P3, HLA-DQ2.2 but not HLA-DQ2.5, showed preferential binding of the serine and threonine variants (14). An earlier study had indicated that HLA-DQ2.2, in contrast to HLA-DQ2.5, utilizes a P3 anchor (20), and a P3 anchor selectivity of HLA-DQ2.2 for serine or threonine was demonstrated when comparing the repertoires of endogenous peptide ligands eluted from purified HLA-DQ2.5, HLA-DQ2.2 and HLA-DQ7.5 molecules (25).

The HLA-DQ2 molecules, HLA-DQ2.5 and HLA-DQ2.2 are highly homologous. Previous studies have ascribed the differences in conferred risk associated with CeD as a result of the polymorphism in the DQα-chain between HLA-DQ2.5 and HLA-DQ2.2 (14,16). In particular, the Tyr22α to Phe22α polymorphism is located near the P3 peptide binding pockets of the HLA-DQ molecule. Here, we examined the role of Phe22α variant in HLA-DQ2.2 that influence peptide binding preferences and how the TCRs derived from DQ2.2 CeD patients engage the HLA-DQ2.2:DQ2.2-glut-L1 complex. We provide a molecular basis for these key interactions in HLA-DQ2.2-mediated CeD and demonstrate how this is different from HLA-DQ2.5- and HLA-DQ8-mediated epitope presentation and TCR recognition in CeD.

Results

DQ2.2-glut-L1-specific TCR repertoire

We performed high-throughput DNA sequencing of rearranged TRAV and TRBV genes of the single HLA-DQ2.2:DQ2.2-glut-L1 tetramer binding CD4^{+} T cells isolated from six T cell lines (TCLs) of four CeD patients described in a previous study (14), specifically CD555 (TCL555.A.1.4 and TCL555.A.2.2), CD594 (TCL594.5.2 and TCL594.8.1), CD627 (TCL627.7.3) and CD1005 (TCL1005.1). Following processing of sequencing data, we

obtained productive paired TCRαβ sequences of 549 cells that were categorized into 18 unique clonotypes (**Table 1**). Cells expressing paired identical nucleotide TRAV/TRBV genes are defined as a clonotype. We also obtained five unique clonotypes by sequencing TRAV/TRBV gene sequences of the T cell clones generated from the same four patients. Of those five unique clonotypes, cells expressing the same TCR as that of three unique T cell clones were observed as clonally expanded population in the single-cell TRAV/TRBV sequencing data generated by tetramer-based sorting. In total, we generated 20 unique clonotypes of DQ2.2-glut-L1-specific T cells from tetramer-sorted single cells and DQ2.2-glut-L1-specific T cell clones.

We observed that few clonotypes dominate the DQ2.2-glut-L1-specific TCR repertoire in the TCLs derived from HLA-DQ2.2 positive CeD patients. In the majority of the patients, one or two expanded clonotypes dominated the T cell repertoire. However, we cannot exclude that some of this bias is the effect of *in vitro* culture of the TCLs. As the number of unique DQ2.2-glut-L1-specific TCRs is small and the data set is obtained from TCLs generated by *in vitro* culture, caution should be exercised on generalizing features of the DQ2.2-glut-L1-specific TCR repertoire. In our fairly limited dataset, we observed that while some V-genes like *TRAV21*, *TRAV26-1*, *TRBV20-1* and *TRBV7-2/3* genes were expressed in more than one CeD patient, there was no apparent V-gene bias, preferential *TRAV:TRBV* pairing or conserved CDR3 features in DQ2.2-glut-L1-specific TCR repertoire. In two patients (CD1005, CD555), we observed T cells expressing TCRs with identical CDR3α and CDR3β amino acid sequences. The CDR3 of these public TCRs are encoded by different nucleotides, representing a phenomenon termed convergent recombination (26).

Among these HLA-DQ2.2:DQ2.2-glut-L1 specific T cell clones, four TCRs were expressed and successfully refolded: TCR 555 (*TRAV1-1*01/TRBV6-2*01*), TCR 594 (*TRAV9-2*01/TRBV11-2*01*), TCR 627 (*TRAV3*01/TRBV28*01*) and TCR 1005.2.56 (*TRAV21*02/TRBV7-3*01*) (**Table 1 & Table S1**). These four HLA-DQ2.2-glut-L1 reactive TCRs do not contain a conserved arginine residue in the CDR loops that underpin the response to gluten antigens in HLA-DQ2.5:DQ2.5-glia-α2, HLA-DQ8:DQ8-glia-α1 and HLA-DQ8:DQ8.5-glia-γ1 reactive TCRs, and displayed more diverse *TRAV/TRBV* gene usage (22,27).

Structural overview of two TCR:HLA-DQ2.2:DQ2.2-glut-L1 complexes

To establish how TCRs interacts with HLA-DQ2.2:DQ2.2-glut-L1, we determined the structure of the TCR 594:HLA-DQ2.2:DQ2.2-glut-L1 and TCR 1005.2.56:HLA-DQ2.2:DQ2.2-glut-L1 ternary complexes at 2.8 Å and 3.0 Å resolution, respectively (**Figure 1, Table S2**). The TCR 594 docked centrally above HLA-DQ2.2:DQ2.2-glut-L1, approximately 85° across the antigen-binding cleft, where the Vα and Vβ chains of the TCR lay above the β- and α-helix of HLA-DQ2.2, respectively (**Figure 1A, 1C**). The total buried surface area (BSA) upon ligation of TCR 594 with HLA-DQ2.2:DQ2.2-glut-L1 was ~1900 Å^2. The Vα and Vβ domains of the TCR 594 contributed 45.4% and 54.6%, respectively, to the BSA at the interface (**Figure 1C**). Notably 36.5% BSA arose from the CDR3β loop, which played a dominant role in contacting the epitope and HLA-DQ2.2 (**Figure 1C**). There was a relatively even distribution of contacts among the CDR loops towards the HLA-DQ2.2 molecule, with the CDR1α, CDR2α and CDR3α and CDR2β loops, contributing 16.4%, 13.6%, 11.2% and 14.1% BSA to the interface, respectively.

The TCR 594 α-chain interacted with the HLA-DQ2.2 β-chain, spanning from Asp66β to Arg80β (**Figure 2A, Table S3**). Here, Tyr30α from the CDR1α loop made van der Waals (vdw) contacts with Asp76β and Arg80β of HLA-DQ2.2, while Thr57α and Asn58α from the CDR2α loop made vdw contacts with Glu69β, Arg72β and Ala73β (**Figure 2A**). The neighboring Vα framework residue Lys55α further stabilizes the CDR2α-HLA-DQ2.2 interactions by forming a salt bridge with Asp66β and Glu69β. Regarding the TCR β-chain, the CDR2β loop made the majority of the contacts with the HLA-DQ2.2 α-chain (**Figure 2B**). Namely, multiple vdw contacts between Gln57β, Asn58β, Gly64β from the TCR and the HLA-DQ2.2 residues Lys39α, Gln57α and Thr61α were observed. Moreover, additional vdw contacts were made between the Vβ framework residue Val66β and the HLA-DQ2.2 residue Asp55α (**Figure 2B**). Accordingly, the TCR 594 engaged the HLA-DQ2.2 molecule in a standard docking mode, with varied contributions from each of the germline-encoded CDR loops.

The TCR 1005.2.56 also adopted a canonical docking position at approximately 60° across the antigen-binding cleft (**Figure 1B, 1D**). The total buried surface area (BSA) upon ligation of TCR1005.2.56 with HLA-DQ2.2:DQ2.2-glut-L1- was slightly higher than TCR 594 with

~2030 Å^2, where the contribution of the Vα and Vβ domains of the TCR 1005.2.56 to the BSA at the interface were 43.8% and 56.2%, respectively. The TCR 1005.2.56 CDR loops made relatively even contact across the HLA-DQ2.2:DQ2.2-glut-L1 (**Figure 1D, Figure 3**). However, the TCR 1005.2.56 made contact with the DQ2.2-glut-L1 epitope with both germline encoded CDR1α and non-germline encoded CDR3β loop (**Figure 1D, 3D**), rather than just the CDR3 residues as seen in the TCR594 ternary complex.

Compared to the TCR 594, the CDR1α loop of the TCR 1005.2.56 shifted closer to the peptide antigen (**Fig S2A**), where Tyr37α made contacts with Phe58α and Arg77β from HLA-DQ2.2-glut-L1, as well as forming a hydrogen bond with the main chain of the peptide P3-Ser and vdw interactions with the P2-Phe (**Figure 3A, 3D, Table S4, Table S5**). This further allows the CDR3α loop to make vdw contact with the Asp55α and Phe58α from HLA-DQ2.2 (**Figure 3A**). The CDR2α loop of the TCR 1005.2.56 made similar contacts with the Glu69β, Arg70β and Ala73β from HLA-DQ2.2 through vdw interactions (**Figure 3A**), comparable to the TCR 594 interactions (**Figure 2A**). All three CDRβ loops from the TCR 1005.2.56 also interacted with the HLA-DQ2.2 molecule (**Figure 3B, 3C**). Similar vdw contacts between CDR1β and CDR2β with a stretch of the helix of the HLA-DQ2.2 α-chain were observed (**Figure 3B**). The Vβ framework residue Tyr55β, Ala66β and Asp67β further supported the interactions between CDR1β and CDR2β and the HLA-DQ2.2 by making H-bond with HLA-DQ2.2 residue Gln57α and additional vdw contacts with Thr61α, Ala64α and His68α (**Figure 3B**). The TCR 1005.2.56 CDR3β also made extensive H-bonds with the HLA-DQ2.2 β-chain (**Figure 3C**). Overall, all CDR loops from both Vα and Vβ domains of the TCR 1005.2.56 made a fairly even number of contact with both the HLA-DQ2.2 as well as the DQ2.2-glut-L1 epitope (**Figure 3E**).

DQ2.2-glut-L1 peptide mediated TCR interactions

The DQ2.2-glut-L1 epitope residues that were exposed for TCR contact were P2-Phe, P5-Gln and P7-Gln (**Figure 2C, Table S5**). The non-germline encoded CDR3 loops of the TCR 594 contacted all three positions, contributing to 22% BSA of the peptide HLA interface (**Table S5**). Here, the CDR3α loop made limited contact, interacting only with the P2-Phe in the DQ2.2-glut-L1 peptide (**Figure 2C**). However, there was an intricate network of polar interactions between the Glu112α residue of CDR3α loop, Arg70β of the HLA-DQ2.2 and the

P5-Gln in the DQ2.2-glut-L1 peptide (**Figure 2D**). This P5-Gln of the DQ2.2-glut-L1 peptide also formed a H-bond with Gly109β of the CDR3β loop, and all together, appeared as a focal point for the CDR3 α/β-loops of the TCR 594 on to the HLA-DQ2.2:DQ2.2-glut-L1 (**Figure 2D**).

The TCR 594 interacted with P7-Gln mostly via its CDR3β loop (**Figure 2C, Table S5**). The small glycine residues in the CDR3β loop, namely Gly109β, Gly110β and Gly112β, which flanked the Trp111β permitted close contact with the peptide and formed H-bond with the side chain of P5-Gln and P7-Gln (**Figure 2C & 2D**). The CDR3β loop of the TCR 594 also displayed extensive interactions with the surrounding residues, where Trp111β formed a H-bond with the side-chain of Asn62 on the HLA-DQ2.2 α-chain, while Glu116β formed a H-bond with Asp66 on the HLA-DQ2.2 β-chain (**Figure 2D**). Trp111β of the CDR3β loop made additional vdw contact with HLA-DQ2.2 α-chain at residues Phe58α, Thr61α and Val65α. Further vdw interactions were made between the Gly112β, Gly113β and Thr115β of the CDR3β loop and the HLA-DQ2.2 β-chain including residues Asp66β, Thr61β and Ile67β. Interestingly, the positioning of the Trp111β in the CDR3β of the TCR 594 is analogous to that of the conserved Arg109 found in the CDR3β loop of the HLA-DQ2.5:DQ2.5-glia-α2 reactive TCRs (**Fig S1**), making similar contact to HLA-DQ2.2 residues Phe58α, Thr61α and Asn62α, as well as gluten epitope residues at position P5 and P7 (**Figure 2C & 2D**).

Gly109α and Thr112β from the TCR 1005.2.56 also interacted with gluten epitope residues at position P5 (**Figure 3D & 3E**). However, the overall TCR:peptide interaction was further extended by contacts between the germline-encoded CDR loops and the DQ2.2-glut-L1 peptide residues P2-Phe, P3-Ser, P6-Glu and P8-Pro, including Tyr37α from the CDR1α loop, the Gln57α from the CDR2α loop and Thr37α from the CDR1α loop (**Figure 3D**). Notably, the P7-Gln residue in the TCR1005.2.56:HLA-DQ2.2:DQ2.2-glut-L1 ternary complex was orientated towards the antigen-binding cleft and formed a H-bond with Arg70β from HLA-DQ2.2 (**Figure 3E**), and was not involved in any direct TCR contact. In TCR 594:HLA-DQ2.2:DQ2.2-glut-L1, Arg70β forms a salt-bridge with the Glu112α from the CDR3α loop and made polar contacts with the P5-Gln of the DQ2.2-glut-L1 (**Figure 2D**). In the TCR1005.2.56:HLA-DQ2.2:DQ2.2-glut-L1 ternary complex, however, the HLA-DQ2.2 residue Arg70β had rotated towards the P7 peptide binding pocket, forming H-bond with P7-

Gln, pulling it inwards, while making H-bond with Thr112β and Asp113β from the CDR3β loop of TCR 1005.2.56 (**Figure 3D, 3E**). Overall, the TCR 1005.2.56 contacts with the HLA-DQ2.2:DQ2.2-glut-L1 are more well distributed along the peptide compared to TCR 594 whose interactions focused on the central region of the peptide.

Comparison of HLA-DQ2.2:DQ2.2-glut-L1 and HLA-DQ2.5:DQ2.5-glia-α2

The DQ2.2-glut-L1 native sequence was derived from low molecular weight glutenin protein (PFSQQQQPV) and the TG2 modified peptides (PFSEQEQPV) was used in this study where the P4 and P6 glutamine residues are converted to glutamate (14,24). Crystal structures of HLA-DQ2.5:DQ2.5-glia-α1 and HLA-DQ2.5:DQ2.5-glia-α2 reveal that lysine at position 71 of the HLA-DQ2.5 β-chain is involved in binding of the P4-Glu and P6-Glu (22,23). The electron density map of the DQ2.2-glut-L1 peptide that are recognized by TCR 594 (Figure 4A) and TCR 1005.2.56 (Figure 4B) was unambiguous. A more comprehensive hydrogen bonding network is shown from the view of a TCR for these two ternary complexes in Figure 4C and 4D, corresponding to P1- to P9 residues of the DQ2.2-glut-L1 peptide shown in Figure 4A and 4B. Similar HLA-peptide contacts were observed in HLA-DQ2.2:DQ2.2-glut-L1, where the P4-Glu and P6-Glu are buried deep into the binding pockets, acting as anchor residues, interacting with Tyr9β, Ser30β and Lys71β of the HLA-DQ2.2 (**Figure 4C and 4D**).

Upon superposition, HLA-DQ2.2:DQ2.2-glut-L1 and HLA-DQ2.5.DQ2.5-glia-α2 showed no major structural differences, with an r.m.s.d. of 0.50Å. The HLA-DQ2.2 and HLA-DQ2.5 have identical DQβ chains and differ by ten residues in the DQ α−chain (**Figure 4E, 4F and 4G**). None of these polymorphic residues of HLA-DQ2.2 made direct contact with the DQ2.2-glut-L1 epitope, or with the TCR in both of the TCR 594:HLA-DQ2.2:DQ2.2-glut-L1 and TCR 1005.2.56:HLA-DQ2.2:DQ2.2-glut-L1complexes solved in this study (**Figure 4E and 4F**). The only key polymorphic residue that is in contact with the DQ2.2-glut-L1 peptide is the Phe/Tyr substitution in position 24. Here we clearly show that the presence of P3-Ser in HLA-DQ2.2:DQ2.2-glut-L1 forms a H-bond to side chain of His24α and main chain of Tyr9 α of the HLA-DQ2.2 molecule (**Figure 4E and 4F**). Whereas in HLA-DQ2.5, Tyr22α of HLA-DQ2.5 (Phe22α in the HLA-DQ2.2) H-bonds with the His24α (**Figure 4G**) (22,23). Moreover, these two HLA-DQ2.2:DQ2.2-glut-L1 complexes displayed relatively conserved electrostatic-potential surfaces for TCR interaction (**Figure 4H and 4I**). Hence, such selective P3-Ser peptide binding preferences is attributed to a hydrogen bonding network whose functionality

is differentially influenced by Tyr22α and Phe22α in HLA-DQ2.5 and HLA-DQ2.2, respectively. While the polymorphic Phe22α is located at the base of the HLA peptide binding cleft and has no direct contact with the TCR, it provides a basis for understanding why P3-Ser binds more favorably to HLA-DQ2.2 compared to HLA-DQ2.5. These structural data are in keeping with a model previously presented (14).

Role of P3-Ser as an anchor in peptide binding to HLA-DQ2.2

To further investigate the role of P3-ser as an anchor residue for HLA-DQ2.2, we performed a competitive peptide binding assay and compared the binding of DQ2.2-glut-L1 and 10 different P3-Ser substituted peptide variants (**Table S6**) to HLA-DQ2.2 **(Figure 5)**. We contrasted the results with testing the same peptides for binding to HLA-DQ2.5 **(Figure 5)**.

Among all the 11 peptides with different amino acids at P3 of the DQ2.2-glut-L1 epitope, the peptide containing P3-Ser displayed the best binding to HLA-DQ2.2. Between the ten P3-Ser substituted peptides, threonine substitution had the least impact. The variant with cysteine also was a reasonable binder. A possible explanation why threonine and cysteine could serve as P3 anchors for HLA-DQ2.2 could be that their side chain, can establish the above-mentioned H-bond to the side chain of His24α and the main chain of Tyr9α. Further to this notion, α-aminobutyric acid which is structurally similar to serine except for lacking the hydroxyl group, bound less well than the serine variant. Notwithstanding, α-aminobutyric acid was better than many of the other amino acids tested indicating additional importance of size and hydrophobicity for optimal anchoring into the P3 pocket of HLA-DQ2.2. The patterns of binding of the 11 DQ2.2-glut-L1 variants to HLA-DQ2.5 was very different for that of HLA-DQ2.2 with P3-Ser not being preferred. Taken together, the binding experiments substantiate the notion of P3-Ser as a key anchor for peptide binding to HLA-DQ2.2 with the hydroxyl group of the serine side being functionally important.

TCR affinity measurements for the HLA-DQ2.2:DQ2.2-glut-L1 complex

As determined by surface plasmon resonance (SPR), the steady-state affinity (K_D) of the TCR 555, 594 and TCR 1005.2.56 for the HLA-DQ2.2:DQ2.2-glut-L1 were 26.14 ± 2.64, 20.95 ± 4.06 and 22.17 ± 3.68 μM, respectively (**Figure 6**). These values corroborate previous T cell proliferation studies (14). None of these TCRs tested showed any binding to HLA-DQ2.5:CLIP1 or HLA-DQ2.2:DQ2.2-glia-α2, thereby highlighting the lack of cross-reactivity of these TCRs.

To determine the extent of peptide sensitivity of these TCRs, we generated three peptide-mutants corresponding to the solvent-exposed residues at position P2, P5 and P7 by replacing them with an alanine. The impact of these substitutions was measured by SPR. The PheP2Ala mutation reduced the affinity by at least 10-fold (K_D>200 µM), whereas the GlnP5Ala mutation abolished TCR binding to HLA-DQ2.2-glut-L1. This is consistent with the crystal structure where P5-Gln played a central role in mediating TCR 594 and TCR 1005.2.56 interaction in HLA-DQ2.2:DQ2.2-glut-L1 (**Figure 2C, 2D, 3D, 3E**). The GlnP7Ala mutation abolished the binding of TCR 555 and 594, whereas the TCR 1005.2.56 showed weak binding (K_D>200 µM) to this mutant, suggesting a different mode of interaction with this TCR. Indeed, as shown in the crystal structure, the P7-Gln in the TCR1005.2.56:HLA-DQ2.2:DQ2.2-glut-L1 ternary complex did not make any direct contact with the TCR, contrary to the TCR594:HLA-DQ2.2:DQ2.2-glut-L1 ternary complex (**Figure 3D, 3E**).

Discussion

HLA-DQ2.2 differs from HLA-DQ2.5 and HLA-DQ8 in gluten peptide binding preferences, and CeD risk association. Immunodominant gluten epitopes that binds stably to HLA-DQ2.5 were found to bind unstably to HLA-DQ2.2 and furthermore did not raise T cell responses *in vivo* in CeD patients carrying HLA-DQ2.2 (14,16). Rather T cell clones from CeD patients expressing HLA-DQ2.2 recognized a unique set of gluten epitopes that commonly had a serine residue at position P3 (14,16). Here, we provide a molecular basis for the T cell-mediated response to an HLA-DQ2.2-restricted immunodominant gluten epitope. We show that, in contrast to HLA-DQ2.5 and HLA-DQ8-mediated CeD, a diverse T cell repertoire underpins the response to HLA-DQ2.2 presenting the glut-L1 epitope. Moreover, we provide a structural basis underpinning this diverse TCR usage, by determining the crystal structures of two TCR:HLA-DQ2.2:DQ2.2-glut-L1 complexes.

Several studies have provided insight into TCR recognition of gluten epitopes presented by HLA-DQ2.5, HLA-DQ8 and HLA-DQ8.5. For instance, the HLA-DQ8:DQ8-glia-α1 reactive TCRs exhibit biased *TRAV26-2/TRBV9-1* gene usage (18), and a non-germline-encoded arginine residue in either the CDR3α or CDR3β loop (23,28). Moreover, *TRAV20⁺/TRBV9⁺* TCRs reactive with HLA-DQ8:DQ8-glia-α1 and HLA-DQ8:DQ8.5-glia-γ1 also possessed a key arginine residue in their CDR1α loops (28,29). All *TRAV26-1/TRBV7-2+* TCRs specific

for DQ2.5-glia-α2 had a non-germline-encoded arginine at position 109 of the CDR3β loop, which forms key interactions with the P5-Leu and P7-Tyr residues found within the gliadin epitopes (22). The HLA-DQ2.5:DQ2.5-glia-α1 reactive TCRs also shows biased TCR gene usage, *TRAV4* and *TRBV20-1* or *TRBV29-1* (22,30) , but they do not carry a conserved arginine that is essential for recognition (31,32). Ensuing structural studies have identified specific structural features that provided a basis for the selection of biased TCR usage and the preferential usage of the Arg residue (22,23).

The TCR594:HLA-DQ2.2:DQ2.2-glut-L1 interactions resembled some features of both TCR S2 and TCR S16 that recognized HLA-DQ2.5:DQ2.5-glia-α1 and HLA-DQ2.5:DQ2.5-glia-α2, respectively. Like the S2 TCR, the germline encoded CDRs on the TCR 594 Vα possesses a tyrosine that make similar interactions with the HLA-DQ2 β-chain helix. Contrary to TCR S2, the TCR 594 interaction with the P5-Gln and P7-Gln, was reminiscent of TCR S16 and JR5.1 recognition of the HLA-DQ2.5:DQ2.5-glia-α2 epitope. Here, although the TCR594 did not possess a conserved arginine residue within the CDR3β loop, Trp111β in the CDR3β loop of the TCR 594, played an analogous role, forming extensive interactions with the HLA-DQ2.2:DQ2.2-glut-L1 complex(**Fig S1**). The nature of the contacts between the TCR 594 and the HLA-DQ2.2:DQ2.2-glut-L1 also provided a basis for understanding the lack of cross-reactivity towards HLA-DQ2.5:DQ2.5-glia-α2. Indeed, the HLA-DQ2.2:DQ2.2-glut-L1 reactive TCRs studied here appeared to be epitope-specific and epitope-driven.

The TCR1005.2.56-HLA-DQ2.2-glut-L1 interactions, on the other hand, resembled TCR Bel502 and Bel602 that recognized HLA-DQ8-glia-α1 and HLA-DQ8-glia-γ1, respectively (28,29) (**Fig S2**). Here, TCR Bel502 and Bel602 possess a conserved Arg37 in the CDR1α loop that interacts with the backbone of the gliadin peptide near the N-termini. The TCR 1005.2.56, like TCR 594, did not bear an arginine in the CDR3β loop nor in the CDR1α loop. However, the Tyr37α in the CDR1α loop of the TCR1005.2.56 sat atop of the N-terminus of the DQ2.2-glut-L1 epitope in the same manner as the conserved Arg37α in the CDR1α loop of TCR Bel502 and Bel602 (**Fig S2B**).

Despite HLA-DQ2.2 compensating for the substitution of Tyr22α by selectively binding to gluten-epitopes with P3-Ser, it bears a lower risk of CD in comparison to HLA-DQ2.5. A higher chance of proteolytic degradation and stricter binding requirements are likely what

limits the repertoire of potential HLA-DQ2.2 epitopes. In addition, the DQ2.2-glut-L1 has a chymotrypsin cleavage site between its P2 and P3 residues, making it more susceptible to proteolytic degradation. The requirement of the deamidation of glutamine residues at P4 and/or P6 for optimal binding to HLA-DQ2.2 further also limits the number of candidate antigenic epitopes in gluten for individuals with this allomorph. These restrictions likely limit the bioavailability of epitopes that could bind to HLA-DQ2.2.

In summary, we have investigated the structural basis of how HLA-DQ2.2-restricted and CeD derived TCRs bind to HLA-DQ2.2 complexed with the immunodominant DQ2.2-glut-L1 peptide. The single polymorphic residue in HLA-DQ2.2 (Phe22α) influences the hydrogen bond network within the peptide-binding groove of HLA-DQ2.2 and selectively bind to gluten epitopes that carry a P3-serine as anchor residue. What is remarkable is that while the TCR-accessible features of the antigen-binding clefts of HLA-DQ2.5 and HLA-DQ2.2 are very similar, the nature of the bound epitopes generate markedly different responding TCR repertoires. In HLA-DQ2.5 mediated CeD, the response is characterized by biased TCR usage, while in HLA-DQ2.2 mediated CeD, a diverse TCR response is generated. Thus, relatively subtle differences in the peptide-centric atomic landscape can have profound effects on the ensuing T cell response, which is correlated with disease pathogenesis.

Methods

Patient material

We characterized T cells isolated from gut biopsy derived T cell lines of four DQ2.2$^+$ subjects that have been described previously (14). According to the Oslo definitions of celiac disease and related terms (33), three of these subjects (CD555, CD594 and CD627) fulfilled the criteria of CeD while one subject (CD1005) fulfilled the criteria of potential CeD having normal gut histology but highly positive anti-transglutaminase 2 (TG2) serology. The subjects gave written informed consents for participation in the previous study, and updated written informed consent forms were obtained for this study. The responsible clinicians had access to sensitive patient data, whereas the research was done on coded material. The study protocol was approved by the Regional Ethical Committee (South East) for Medical and Health Research Ethics (present project ID: 6544). From the T cell lines we sorted single T cells with HLA-DQ tetramers for TCR sequencing and TCRs of already established T cell clones were sequenced (TCC627.1.3.199, TCC594.5.2.6 and TCC555A.1.4.38 from ref. (14) and TCC1005.2.54,

TCC1005.2.56, TCC1005.2.57, TCC1005.2.58, TCC1005.2.60, TCC1005.2.62, and TCC1005.2.65 from ref.(34).

Tetramer staining, surface antibody staining and fluorescence-activated cell sorting (FACS)

Tetramers of recombinant HLA-DQ2.2 covalently linked with DQ2.2-glut-L1 peptide (QP<u>PFSEQEQPVL</u>, underlined 9-mer core amino acid sequence) and CLIP1 (PVSK<u>MRMATPLLM</u>QA, negative control for non-specific binding) were produced as per Dorum, et al. (24) and conjugated with phycoerythrin-labeled streptavidin (Invitrogen) and allophycocyanin-labeled streptavidin (ProZyme), respectively. Cryopreserved T cell lines were thawed and stained with PE conjugated HLA-DQ2.2:DQ2.2-glut-L1 (10 µg/ml) and APC conjugated HLA-DQ2.2: CLIP1 (10 µg/ml) for 2 hours at 37°C. Following tetramer staining, the cells were stained with the mix of surface antibodies for FACS. We sorted live, singlets that were CD3$^+$, CD8$^-$, CD4$^+$, HLA-DQ2.2:DQ2.2-glut-L1 tetramer$^+$ and HLA-DQ2.2:CLIP1 tetramer$^-$ (**Fig S3**). The cells were sorted in 96-well plate containing lysis buffer for single-cell TCR sequencing. The sorting was performed with a FACS Aria II instrument (BD Biosciences) at the Flow Cytometry Core Facility (Oslo University Hospital) and the flow cytometry data was analyzed with FlowJo software (FlowJo LLC). The following antibodies were used in the study: CD3-Superbright 600 (eBioscience), CD4-APC-H7 (BD Biosciences) and CD8-PerCP (eBioscience). LIVE/DEAD marker fixable violet stain (Thermo Fischer Invitrogen) was used to exclude dead cells.

TCR sequencing of T cell clones

Sequences of rearranged TCR-α and TCR-β genes of T cell clones were obtained by Sanger sequencing using a protocol as described (35).

Single-cell TCR gene sequencing and processing of TCR gene sequences

We used a previously published protocol, based on nested PCR amplification using multiplex *TRAV* and *TRBV* primers, for single-cell TCRαβ sequencing (3,36). The processing of the raw sequences generated from Illumina NGS was carried out as described (3). Sequencing was performed using Illumina MiSeq (250 bp PE) platform at the Norwegian Sequencing Centre (Oslo University Hospital).

Competitive peptide binding assays

The competitive peptide binding assay was performed as described previously (37) (38). In brief, the EBV-transformed B-cell lines VAVY (#9023) and MOU (#9050) were used as the source of HLA-DQ2.5 and HLA-DQ2.2 molecules. Microtiter plates (96 well, Nunc) were coated with an anti-DQ mAb (mAbSPV-L3; 2μg per well) as capture antibody for overnight at 4°C. The wells were then blocked with PBS/gelatin (0.2%) at 37 °C for 5 hours. The plates were washed and cell lysate of EBV cells (equivalent of 4 million cells) was added to wells and incubated at 4°C overnight. The plates were washed and biotinylated indicator peptide P418 (EPRAPWIEQEGPEYW-biotin, 0.5μM) together with unlabeled competitor peptides (GL Biochem (Shanghai) were added in binding buffer with protease inhibitors (Complete EDTA-free tablets, Roche Molecular Biochemicals) and 1mM DTT followed by 48 hours incubation at 37°C. The plates were washed and incubated with streptavidin-europium diluted (1000x dilution) in DELFIA assay buffer (Wallac) for 45 minutes at room temperature. The plates were washed and incubated with DELFIA enhancement solution (Wallac) for 15 minutes at room temperature. Binding of the indicator peptide was then measured as Eu counts in a time-resolved fluorometer (Wallac 1420 multilabel counter). IC_{50} values (the concentration of the competitor peptide required for half-maximal inhibition of the binding of the indicator peptide) were established for each peptide. One 10-fold titration experiment and three 4-fold titration experiments were performed. The relative binding capacity was calculated as the ratio of the IC_{50} value of the DQ2.2-glut-L1 to the IC_{50} value of the P3-substituted peptide variants.

Protein expression and purification

cDNAs (Genscript) encoding the individual extracellular domains of TCR α and β chains, with an engineered interchain disulfide linkage in the constant domains were cloned into the pET-30 vector and expressed in *E. coli* BL21DE3. The TCR proteins were purified from inclusion bodies, as described previously (39,40). The TCR αβ heterodimers were refolded in the presence of 5M Urea, followed by dialysis and further purification through anion exchange chromatography, size-exclusion chromatography, hydrophobic-interaction chromatography as described previously (18).

For SPR and structural experiments, the extracellular domains of the HLA-DQ2.2 α-chain and HLA-DQ2.2-glut-L1 β-chain (with glut-L1 epitope covalently linked to the HLA-DQ2.2 β-chain) were co-expressed as soluble protein in High Five insect cells (*Trichoplusia ni* BTI-TN-5B1-4 cells; Invitrogen), via a baculovirus expression system as described previously (17).

Briefly, baculovirus HLA-DQ2.2 expression constructs had enterokinase-cleavable Fos and Jun zippers at the C-terminal ends of the α- and β-chain, respectively, to promote dimerization. The C terminus of the β-chain also included a BirA recognition sequence for biotinylation, as described previously (18), as well as a histidine tag for purification using immobilized metal ion affinity chromatography. Before crystallization, the Fos and Jun zippers were removed by enterokinase (Genscript) digestion, followed by separation using anion exchange chromatography (HiTrap Q HP, GE Healthcare). Purified HLA-DQ2.2:DQ2.2-glut-L1 was mixed in a 1:1 ratio with purified TCR 594 or TCR 1005.2.56, and the protein complex was then purified by size exclusion chromatography (Superdex 200; GE Healthcare). Three HLA-DQ2.2-glut-L1 epitope mutants were generated by replacing the glut-L1 wild type (WT) core sequence (PFSEQEQPV) with glut-L1-P2Δ (PASEQEQPV), glut-L1-P5Δ (PFSEAEQPV) and glut-L1-P7Δ (PFSEQEAPV) separately in the HLA-DQ2.2 β-chain, and co-expressed with HLA-DQ2.2 α-chain via a baculovirus expression system as described above.

Crystallization, data collection and processing

The TCR 594/TCR 1005.2.56 and the HLA-DQ2.2:DQ2.2-glut-L1 complex, in 10mM Tris (pH 8), 150mM NaCl, were concentrated to 6 mg/ml. Crystallization was carried out using the hanging-drop vapor-diffusion method at 17 °C. For TCR594:HLADQ2.2:DQ2.2-glut-L1, diffraction quality crystal was obtained in conditions 0.1 M MES pH 6.5, 5% v/v MPD and 15% w/v PEG6K, and crystallization droplets were set up by adding 1 μl of the mother liquor to 1 μl of protein solution. Crystals typically appeared within 2–7 d. For TCR1005.2.56:HLA-DQ2.2:DQ2.2-glut-L1, diffraction quality crystal was obtained in an optimized Morpheus screen conditions 0.1 M MOPS/HEPES pH 7.5, 12.5% v/v PEG1K, 12.5% v/v MPD, 12.5% w/v PEG3350 and 0.04 M NPS mixture (41), and crystallization droplets were set up by adding 1 μl of the mother liquor to 1 μl of protein solution and with the addition of 0.2 μl of seed stock. Crystals typically appeared within 2-3 weeks. Protein crystals were exposed to cryoprotectant, 20% glycerol for 30 s before being flash-cooled in liquid nitrogen. Data sets were collected on the MX2 beamline of the Australian Synchrotron. Data was integrated with XDS and scaled and merged in Aimless. Phases were obtained using molecular replacement in PhaserMR, CCP4suite (42). The PDB entry 4OZH (chain A and B, without glycans or peptides for MHC; chain G and H for TCR) was used as search model for HLA-DQ2.2:DQ2.2-glut-L1 and TCR 594 for molecular replacement. The data collected for the TCR594:HLADQ2.2:DQ2.2-glut-L1was highly anisotropic, thus ellipsoidal truncations and anisotropic scaling were carried out

at the Diffraction Anisotropic Server (43). The structure was built and refined in Coot and PHENIX (44,45). Final model was validated in Molprobity (45).

Surface plasmon resonance measurement and analysis

Surface plasmon resonance experiments were conducted on a BIAcore^{TM} T200 system (GE Healthcare Life Sciences) instrument using HBS buffer (10 mM HEPES-HCl, pH 7.4, 150 mM NaC l and 0.005% surfactant P20). The biotinylated HLA-DQ2.5:CLIP2, HLA-DQ2.2:DQ2.2-glut-L1 and respective peptide mutant DQ2.2-glut-L1-P2Δ, DQ2.2-glut-L1-P5Δ, DQ2.2-glut-L1-P7Δ were immobilized on a streptavidin-coated Biacore Series S Sensor Chip SA (SA Chip; GE Healthcare Life Sciences), creating a surface density of approximately 800-1000 response units (RU). The TCR 555, 594 and 1005.2.56 (1 in 2 serial dilutions from the maximum concentration of 200 uM) were injected over the chip at 10 μl/min for 2 min. The TCR response to HLA-DQ2.5:CLIP2 alone was subtracted from the response to HLA-DQ2.2:DQ2.2-glut-L1 and respective epitope mutants. Data in the main text are representative of two or four independent experiments. The equilibrium dissociation constant, K_D, were generated with nonlinear regression analysis of the combined data using Prism (GraphPad Software).

Data Availability

The protein structural data that support the findings of this study have been deposited in the RCSB Protein Data Bank with the accession codes 6PX6 and 6PY2. All the single-cell TCR sequencing raw data generated in this study are available in the European Genome-phenome Archive (EGAS00001003673).

Author contributions

YTT, SDK and SWQ contributed to data generation and analysis and prepared the manuscript. HSKK, RN, KEAL and JP contributed to data generation and reviewed the manuscript. HHR, LMS and JR conceived the study, contributed to data analysis, and prepared the manuscript.

Competing Interests

The authors declare that the research was conducted in the absence of any commercial or financial relationships that could be construed as a potential conflict of interest.

References

1. Abadie, V., Sollid, L. M., Barreiro, L. B., and Jabri, B. (2011) Integration of genetic and immunological insights into a model of celiac disease pathogenesis. *Annual review of immunology* **29**, 493-525

2. Molberg, O., Kett, K., Scott, H., Thorsby, E., Sollid, L. M., and Lundin, K. E. (1997) Gliadin specific, HLA DQ2-restricted T cells are commonly found in small intestinal biopsies from coeliac disease patients, but not from controls. *Scand J Immunol* **46**, 103-109

3. Risnes, L. F., Christophersen, A., Dahal-Koirala, S., Neumann, R. S., Sandve, G. K., Sarna, V. K., Lundin, K. E., Qiao, S. W., and Sollid, L. M. (2018) Disease-driving CD4+ T cell clonotypes persist for decades in celiac disease. *J Clin Invest* **128**, 2642-2650

4. Sollid, L. M., and Jabri, B. (2013) Triggers and drivers of autoimmunity: lessons from coeliac disease. *Nature Reviews Immunology* **13**, 294

5. Jabri, B., and Sollid, L. M. (2017) T cells in celiac disease. *The Journal of Immunology* **198**, 3005-3014

6. Sollid, L. M., Markussen, G., Ek, J., Gjerde, H., Vartdal, F., and Thorsby, E. (1989) Evidence for a primary association of celiac disease to a particular HLA-DQ alpha/beta heterodimer. *J Exp Med* **169**, 345-350

7. Sollid, L. M. (2000) Molecular basis of celiac disease. *Annu Rev Immunol* **18**, 53-81

8. Fleckenstein, B., Molberg, Ø., Qiao, S.-W., Schmid, D. G., von der Mülbe, F., Elgstøen, K., Jung, G., and Sollid, L. M. (2002) Gliadin T Cell Epitope Selection by Tissue Transglutaminase in Celiac Disease ROLE OF ENZYME SPECIFICITY AND pH INFLUENCE ON THE TRANSAMIDATION VERSUS DEAMIDATION REACTIONS. *Journal of Biological Chemistry* **277**, 34109-34116

9. Vader, L. W., de Ru, A., van der Wal, Y., Kooy, Y. M., Benckhuijsen, W., Mearin, M. L., Drijfhout, J. W., van Veelen, P., and Koning, F. (2002) Specificity of tissue transglutaminase explains cereal toxicity in celiac disease. *Journal of Experimental Medicine* **195**, 643-649

10. Xia, J., Sollid, L. M., and Khosla, C. (2005) Equilibrium and kinetic analysis of the unusual binding behavior of a highly immunogenic gluten peptide to HLA-DQ2. *Biochemistry* **44**, 4442-4449

11. Molberg, O., McAdam, S. N., Korner, R., Quarsten, H., Kristiansen, C., Madsen, L., Fugger, L., Scott, H., Noren, O., Roepstorff, P., Lundin, K. E., Sjostrom, H., and Sollid, L. M. (1998) Tissue transglutaminase selectively modifies gliadin peptides that are recognized by gut-derived T cells in celiac disease. *Nat Med* **4**, 713-717

12. van de Wal, Y., Kooy, Y., van Veelen, P., Peña, S., Mearin, L., Papadopoulos, G., and Koning, F. (1998) Cutting edge: selective deamidation by tissue transglutaminase strongly enhances gliadin-specific T cell reactivity. *The Journal of Immunology* **161**, 1585-1588

13. Qiao, S. W., Bergseng, E., Molberg, O., Jung, G., Fleckenstein, B., and Sollid, L. M. (2005) Refining the rules of gliadin T cell epitope binding to the disease-associated DQ2 molecule in celiac disease: importance of proline spacing and glutamine deamidation. *Journal of immunology (Baltimore, Md. : 1950)* **175**, 254-261

14. Bodd, M., Kim, C. Y., Lundin, K. E., and Sollid, L. M. (2012) T-cell response to gluten in patients with HLA-DQ2. 2 reveals requirement of peptide-MHC stability in celiac disease. *Gastroenterology* **142**, 552-561

15. Tollefsen, S., Arentz-Hansen, H., Fleckenstein, B., Molberg, O., Raki, M., Kwok, W. W., Jung, G., Lundin, K. E., and Sollid, L. M. (2006) HLA-DQ2 and -DQ8 signatures of gluten T cell epitopes in celiac disease. *J Clin Invest* **116**, 2226-2236

16. Fallang, L.-E., Bergseng, E., Hotta, K., Berg-Larsen, A., Kim, C.-Y., and Sollid, L. M. (2009) Differences in the risk of celiac disease associated with HLA-DQ2. 5 or HLA-DQ2. 2 are related to sustained gluten antigen presentation. *Nature immunology* **10**, 1096

17. Henderson, K. N., Tye-Din, J. A., Reid, H. H., Chen, Z., Borg, N. A., Beissbarth, T., Tatham, A., Mannering, S. I., Purcell, A. W., and Dudek, N. L. (2007) A structural and immunological basis for the role of human leukocyte antigen DQ8 in celiac disease. *Immunity* **27**, 23-34

18. Broughton, S. E., Petersen, J., Theodossis, A., Scally, S. W., Loh, K. L., Thompson, A., van Bergen, J., Kooy-Winkelaar, Y., Henderson, K. N., and Beddoe, T. (2012) Biased T cell receptor usage directed against human leukocyte antigen DQ8-restricted gliadin peptides is associated with celiac disease. *Immunity* **37**, 611-621

19. Johansen, B. H., Jensen, T., Thorpe, C. J., Vartdal, F., Thorsby, E., and Sollid, L. M. (1996) Both alpha and beta chain polymorphisms determine the specificity of the disease-associated HLA-DQ2 molecules, with beta chain residues being most influential. *Immunogenetics* **45**, 142-150

20. van de Wal, Y., Kooy, Y. M., Drijfhout, J. W., Amons, R., Papadopoulos, G. K., and Koning, F. (1997) Unique peptide binding characteristics of the disease-associated DQ (α1* 0501, β1* 0201) vs the non-disease-associated DQ (α1* 0201, β1* 0202) molecule. *Immunogenetics* **46**, 484-492

21. Kim, C.-Y., Quarsten, H., Bergseng, E., Khosla, C., Sollid, L. M., and Strominger, J. L. (2004) Structural Basis for HLA-DQ2-Mediated Presentation of Gluten Epitopes in Celiac Disease. *Proceedings of the National Academy of Sciences of the United States of America* **101**, 4175-4179

22. Petersen, J., Montserrat, V., Mujico, J. R., Loh, K. L., Beringer, D. X., Van Lummel, M., Thompson, A., Mearin, M. L., Schweizer, J., and Kooy-Winkelaar, Y. (2014) T-cell receptor recognition of HLA-DQ2–gliadin complexes associated with celiac disease. *Nature Structural and Molecular Biology* **21**, 480

23. Petersen, J., van Bergen, J., Loh, K. L., Kooy-Winkelaar, Y., Beringer, D. X., Thompson, A., Bakker, S. F., Mulder, C. J., Ladell, K., and McLaren, J. E. (2015) Determinants of gliadin-specific T cell selection in celiac disease. *The Journal of Immunology* **194**, 6112-6122

24.   Dørum, S., Bodd, M., Fallang, L.-E., Bergseng, E., Christophersen, A., Johannesen, M. K., Qiao, S.-W., Stamnaes, J., de Souza, G. A., and Sollid, L. M. (2014) HLA-DQ molecules as affinity matrix for identification of gluten T cell epitopes. *The Journal of Immunology* **193**, 4497-4506

25.   Bergseng, E., Dorum, S., Arntzen, M. O., Nielsen, M., Nygard, S., Buus, S., de Souza, G. A., and Sollid, L. M. (2015) Different binding motifs of the celiac disease-associated HLA molecules DQ2.5, DQ2.2, and DQ7.5 revealed by relative quantitative proteomics of endogenous peptide repertoires. *Immunogenetics* **67**, 73-84

26.   Venturi, V., Price, D. A., Douek, D. C., and Davenport, M. P. (2008) The molecular basis for public T-cell responses? *Nature reviews. Immunology* **8**, 231-238

27.   Jabri, B., Chen, X., and Sollid, L. M. (2014) How T cells taste gluten in celiac disease. *Nature Structural and Molecular Biology* **21**, 429

28.   Petersen, J., Kooy-Winkelaar, Y., Loh, K. L., Tran, M., Van Bergen, J., Koning, F., Rossjohn, J., and Reid, H. H. (2016) Diverse T cell receptor gene usage in HLA-DQ8-associated celiac disease converges into a consensus binding solution. *Structure (London, England : 1993)* **24**, 1643-1657

29.   Rossjohn, J., and Koning, F. (2016) A biased view toward celiac disease. *Mucosal Immunology* **9**, 583

30.   Dahal-Koirala, S., Ciacchi, L., Petersen, J., Risnes, L. F., Neumann, R. S., Christophersen, A., Lundin, K. E. A., Reid, H. H., Qiao, S. W., Rossjohn, J., and Sollid, L. M. (2019) Discriminative T-cell receptor recognition of highly homologous HLA-DQ2-bound gluten epitopes. *J Biol Chem* **294**, 941-952

31.   Qiao, S.-W., Christophersen, A., Lundin, K. E., and Sollid, L. M. (2013) Biased usage and preferred pairing of α-and β-chains of TCRs specific for an immunodominant gluten epitope in coeliac disease. *International immunology* **26**, 13-19

32.   Qiao, S.-W., Ráki, M., Gunnarsen, K. S., Løset, G.-Å., Lundin, K. E. A., Sandlie, I., and Sollid, L. M. (2011) Posttranslational Modification of Gluten Shapes TCR Usage in Celiac Disease. *The Journal of Immunology* **187**, 3064-3071

33.   Ludvigsson, J. F., Leffler, D. A., Bai, J. C., Biagi, F., Fasano, A., Green, P. H. R., Hadjivassiliou, M., Kaukinen, K., Kelly, C. P., Leonard, J. N., Lundin, K. E. A., Murray, J. A., Sanders, D. S., Walker, M. M., Zingone, F., and Ciacci, C. (2013) The Oslo definitions for coeliac disease and related terms. *Gut* **62**, 43

34.   Dorum, S., Bodd, M., Fallang, L. E., Bergseng, E., Christophersen, A., Johannesen, M. K., Qiao, S. W., Stamnaes, J., de Souza, G. A., and Sollid, L. M. (2014) HLA-DQ molecules as affinity matrix for identification of gluten T cell epitopes. *Journal of immunology (Baltimore, Md. : 1950)* **193**, 4497-4506

35.   Dahal-Koirala, S., Risnes, L. F., Christophersen, A., Sarna, V. K., Lundin, K. E., Sollid, L. M., and Qiao, S. W. (2016) TCR sequencing of single cells reactive to DQ2.5-glia-alpha2 and DQ2.5-glia-omega2 reveals clonal expansion and epitope-specific V-gene usage. *Mucosal Immunol* **9**, 587-596

36.   Han, A., Glanville, J., Hansmann, L., and Davis, M. M. (2014) Linking T-cell receptor sequence to functional phenotype at the single-cell level. *Nat Biotechnol* **32**, 684-692

37.   Bodd, M., Kim, C. Y., Lundin, K. E. A., and Sollid, L. M. (2012) T-Cell Response to Gluten in Patients With HLA-DQ2.2 Reveals Requirement of Peptide-MHC Stability in Celiac Disease. *Gastroenterology* **142**, 552-561

38.   Vader, W., Stepniak, D., Kooy, Y., Mearin, L., Thompson, A., van Rood, J. J., Spaenij, L., and Koning, F. (2003) The HLA-DQ2 gene dose effect in celiac disease is directly related to the magnitude and breadth of gluten-specific T cell responses. *Proc Natl Acad Sci U S A* **100**, 12390-12395

39. Boulter, J. M., Glick, M., Todorov, P. T., Baston, E., Sami, M., Rizkallah, P., and Jakobsen, B. K. (2003) Stable, soluble T-cell receptor molecules for crystallization and therapeutics. *Protein Engineering, Design and Selection* **16**, 707-711

40. Garboczi, D. N., Ghosh, P., Utz, U., Fan, Q. R., Biddison, W. E., and Wiley, D. C. (1996) Structure of the complex between human T-cell receptor, viral peptide and HLA-A2. *Nature* **384**, 134-141

41. Gorrec, F. (2015) The MORPHEUS II protein crystallization screen. *Acta Crystallogr F Struct Biol Commun* **71**, 831-837

42. Winn, M. D., Ballard, C. C., Cowtan, K. D., Dodson, E. J., Emsley, P., Evans, P. R., Keegan, R. M., Krissinel, E. B., Leslie, A. G., McCoy, A., McNicholas, S. J., Murshudov, G. N., Pannu, N. S., Potterton, E. A., Powell, H. R., Read, R. J., Vagin, A., and Wilson, K. S. (2011) Overview of the CCP4 suite and current developments. *Acta Crystallogr D Biol Crystallogr* **67**, 235-242

43. Strong, M., Sawaya, M. R., Wang, S., Phillips, M., Cascio, D., and Eisenberg, D. (2006) Toward the structural genomics of complexes: Crystal structure of a PE/PPE protein complex from Mycobacterium tuberculosis. *Proceedings of the National Academy of Sciences* **103**, 8060-8065

44. Adams, P. D., Afonine, P. V., Bunkoczi, G., Chen, V. B., Davis, I. W., Echols, N., Headd, J. J., Hung, L. W., Kapral, G. J., Grosse-Kunstleve, R. W., McCoy, A. J., Moriarty, N. W., Oeffner, R., Read, R. J., Richardson, D. C., Richardson, J. S., Terwilliger, T. C., and Zwart, P. H. (2010) PHENIX: a comprehensive Python-based system for macromolecular structure solution. *Acta Crystallogr D Biol Crystallogr* **66**, 213-221

45. Chen, V. B., Arendall, W. B., 3rd, Headd, J. J., Keedy, D. A., Immormino, R. M., Kapral, G. J., Murray, L. W., Richardson, J. S., and Richardson, D. C. (2010) MolProbity: all-atom structure validation for macromolecular crystallography. *Acta Crystallogr D Biol Crystallogr* **66**, 12-21

Figure legends

Fig 1. Structures of TCR- HLA-DQ2.2:DQ2.2-glut-L1 ternary complexes (**A**) TCR 594 and (**B**) 1005.2.56 TCR. Footprint of the CDR loops of the TCR 594 (**C**) and TCR 1005.2.56 (**D**) on the HLA-DQ2.2:DQ2.2-glut-L1. CDR1α, CDR2α and CDR3α are colored in red, pink, and purple, respectively, whilst the CDR1β, CDR2β and CDR3β are colored in green, light teal, and yellow respectively. The TCR framework for each Vα and Vβ are colored orange and brown respectively for TCR 594, and colored lime and deep-olive for TCR 1005.2.56. The pie chart below show percentage of the CDR loops contributing to the buried surface area.

Fig 2. TCR 594 CDR loops in contact with the HLA-DQ2.2:DQ2.2-glut-L1. (**A**) The CDR1α and CDR2α loop contacting HLA-DQ2.2 β-chain. (**B**) The CDR2β contacts with HLA-DQ2.2 α-chain. (**C**) CDR3α and CDR3β interactions with the DQ2.2-glut-L1 peptide. Key interaction around the P5-Gln (**D**) residue of the DQ2.2-glut-L1 epitope.

Fig 3. TCR 1005.2.56 CDR loops in contact with the HLA-DQ2.2:DQ2.2-glut-L1. (**A**) The CDR1α, CDR2α and CDR3α loops contacts the HLA-DQ2.2 α-chain and β-chain. The CDR1β, CDR2β (**B**) and CDR3β (**C**) interactions with the HLA-DQ2.2 α-chain and β-chain respectively. (**D**) The CDR1α and CDR3β loops of the TCR 1005.2.56 that interacted the DQ2.2-glut-L1 peptide. The CDR3α, CDR1β and CDR2β loop contacts with the peptide. (**E**) Key interaction around the P5-Gln and P7-Gln residue of the DQ2.2-glut-L1 epitope.

Fig 4. Comparison of HLA-DQ2.2-glut-L1 and HLA-DQ2.5 in complexed with gluten epitopes. The DQ2.2-glut-L1 peptide is bound in the peptide-binding groove, with carbon colored in salmon, nitrogen colored in blue, and oxygen colored in red. The TCR 594 (**A**) and TCR 1002.56 (**B**) docked on top of the HLA-DQ2.2:DQ2.2-glut-L1 are shown as solid surface and each of the TCR αβ pair were colored in brown/orange and green/lime respectively. The peptide's 2Fo-Fc electron density map is shown in blue and contoured to 1 σ. Hydrogen bond interactions between HLA-DQ2.2 and the DQ2.2-glut-L1 epitope in the TCR 594:HLA-DQ2.2:DQ2.2-glut-L1 ternary complex (**C**) and in the TCR 1005.2.56:HLA-DQ2.2:DQ2.-glut-L1 ternary complex (**D**) are shown. Comparison of the DQ2.2-glut-L1 peptide bound to HLA-DQ2.2 in the two ternary complexes solved showed minor movement in P7-Gln residues, highlighted in yellow circle. Polymorphic residues on the ectodomain of HLA-DQ differing between HLA-DQ2.2 (**E, F**) and HLA-DQ2.5 (**G**) are represented in stick and colored in fire-brick. The His24α interacts with P3-Ser in DQ2.2-glut-L1 (**E, F**) but with Tyr22α in HLA-DQ2.5 (**G**). The solvent-accessible electrostatic potential was calculated for HLA-DQ2.2:DQ2.2-glut-L1 in complexed with TCR 594 (**H**) or TCR 1005.2.56 (**I**) and HLA-DQ2.5:DQ2.5-glia-α-2 (**J**). Electrostatic calculations were performed using APBS (± 5 *kT/e*).

Fig 5. Binding of unsubstituted and P3-susbstituted variants of the DQ2.2-glut-L1 epitope to HLA-DQ2.2 and HLA-DQ2.5. Synthetic peptides containing the DQ2.2-glut-L1 epitope (Ac-QQPPFSEQEQPVLPQ, nine amino acid core sequence underlined) and variants substituted at P3 serine were tested as competitor peptides. The inhibitory effect of the competitor peptides is shown as IC_{50} values. One 10-fold titration experiment and three 4-fold titration experiments were performed. **A** Representative data showing results of one of the three 4-fold titration experiments. **B** Results from all four independents experiments depicted as relative binding capacities (i.e. compared to the unsubstituted DQ2.2-glut-L1 epitope). The relative binding values from each experiment are shown as dots with bars representing mean

values. A missing dot for some peptides is due to the titration curve not reaching its relevant IC_{50} value. Error bars, s.d.

Fig 6. Affinity measurement of TCR 555, 594 and 1005.2.56. Affinity for HLA-DQ2.2:DQ2.2-glut-L1 wild type (WT) and the P2-Ala, P5-Ala and P-7Ala epitope mutants were measure via SPR. 2- 4 independent experiments (with the number of replicates shown as *n* numbers) were carried out for each of the TCR against each of HLA-DQ2.2-glut-L1 wild-type (WT) and epitope mutants. Binding curve showed represent an independent experiment of TCR 555, TCR 594, TCR 1005.2.56 (labeled as TCR256) binding to HLA-DQ2.2:DQ2.2-glut-L1. All data were combined for each TCR and a One-site specific binding model was used for curve fitting. HLA-DQ2.5-CLIP was used as negative control and acted as baseline reference value. RU, response units. Error bars, s.d.

Supplementary Figure legends

Fig S1. Overlay of CDR loops of TCR594 recognizing gluten epitopes bound to HLA-DQ2.2-glut-L1. Overlay of ternary structures: TCR594:HLA-DQ2.2:DQ2.2-glut-L1, PDB 4OZH (TCR S16:HLA-DQ2.5:DQ2.5-glia-α2) and PDB 4OZF (TCR JR5.1:HLA-DQ2.5:DQ2.5-glia-α2). Alignment of these structures showed that the Trp111β on the CDR3β of TCR594 also aligned with the conserved Arg109β in TCR S16:HLA-DQ2.5:DQ2.5-glia-α2 that make conserved contacts with the gluten epitope, as well as both chains from HLA-DQ2 molecule (**A**). The Tyr30α in the CDR1α loop, like the conserved Tyr38α in HLA-DQ2.5:DQ2.5-glia-α1 reactive TCR S16 and JR5.1, make conserved contact to the HLA-DQ2 β-chain (**B**).

Fig S2. Overlay of CDR loops of TCR1005.2.56 recognizing gluten epitopes bound to HLA-DQ2. (A) Overlay of ternary structures: TCR 1005.2.56-HLA-DQ2.2-glut-L1 and TCR594-HLA-DQ2.2-glut-L1. There is a conserved tyrosine in the CDR1α loops of these two TCRs, Tyr30α (TCR 594) and Tyr37α (TCR 1005.2.56) make conserved contact to the HLA-DQ2.2-glut-L1. While the Tyr30α of the TCR594 make essential contact with the HLA-DQ2.2 β-chain, it has shifted closer to the peptide antigen cleft in the TCR 1005.2.56:HLA-DQ2.2-DQ2.2-glut-L1 complex, where it interacts with the backbone of the peptide as well as surrounding HLA-DQ2.2 residues from both α-chain and β-chain. (**B**) Alignment of TCR 1005.2.56 with previously published structures showed that the Tyr37α on the CDR1α of TCR594 aligned with the conserved Arg110α in HLA-DQ8-glia-α1 (PDB: 5KS9) and HLA-DQ8.5-glia-γ1 (PDB: 5KSA) restricted TCRs, Bel502 and Bel602 that make essential contacts with the gluten epitope.

Fig S3. Gating strategy. We sorted single lymphocytes that were live CD3^{+}, CD8^{-}, CD4^{+}, HLA-DQ2.2:CLIP1 tetramer^{-} and HLA-DQ2.2:DQ2.2-glut-L1 tetramer^{+}.

Figure 1.

A TCR 594

Vβ   Vα

α - chain   β - chain

HLA-DQ2.2:DQ2.2-glut-L1

B TCR 1005.2.56

Vβ   Vα

α - chain   β - chain

HLA-DQ2.2:DQ2.2-glut-L1

C

Vβ   DQα

Vα

DQβ

- CDR1a
- CDR2a
- CDR3a
- CDR1b
- CDR2b
- CDR3b
- Fw a
- Fw b

3.8 %
16.4 %
13.6 %
11.2%
4.2 %
14.1 %
36.5%

D

Vβ   DQα

Vα

DQβ

- CDR1a
- CDR2a
- CDR3a
- CDR1b
- CDR2b
- CDR3b
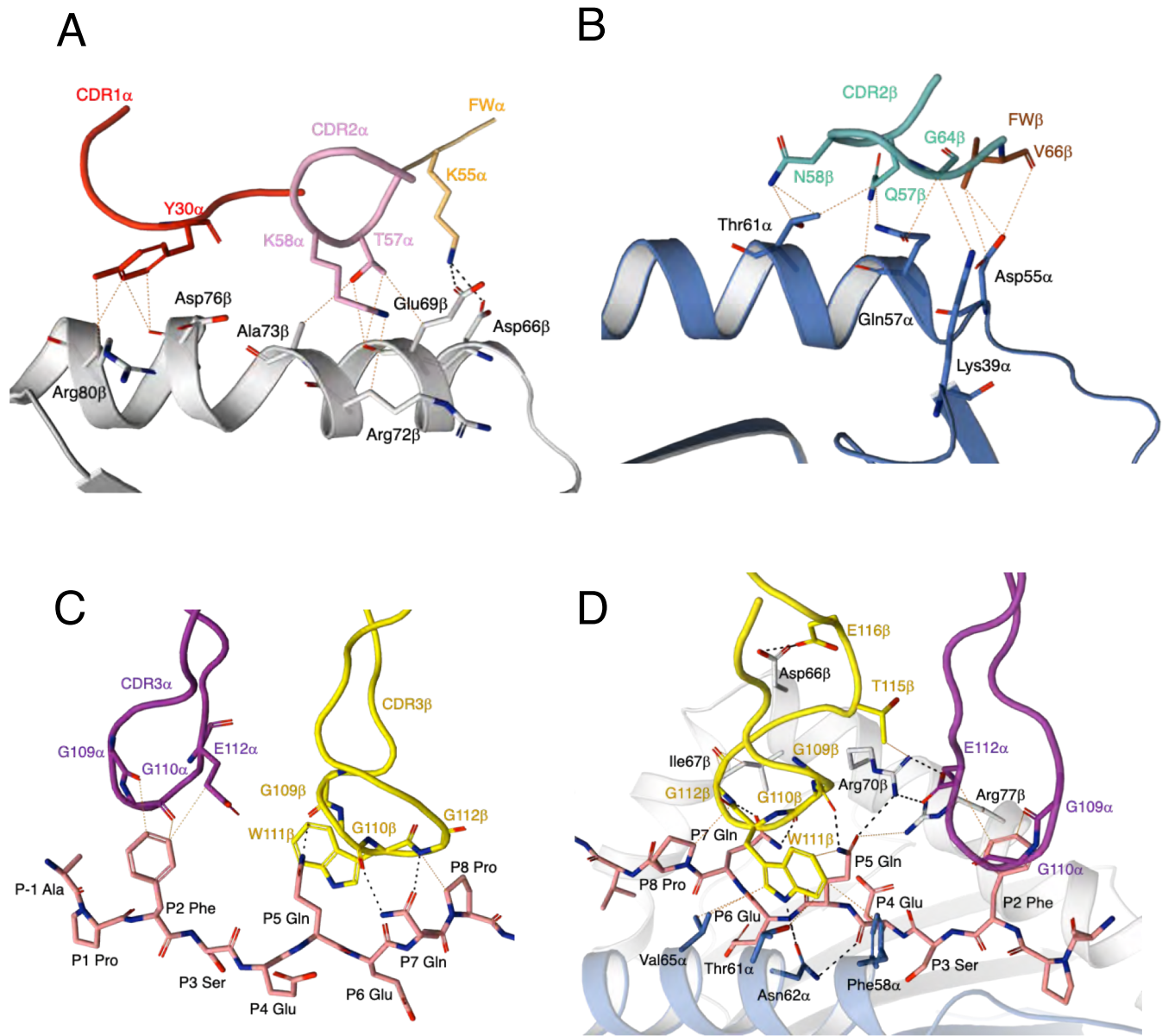- Fw a
- Fw b

13.3 %
17.4 %
16.3 %
7.9 %
3.2 %
6.6 %
9.1 %
27.2%
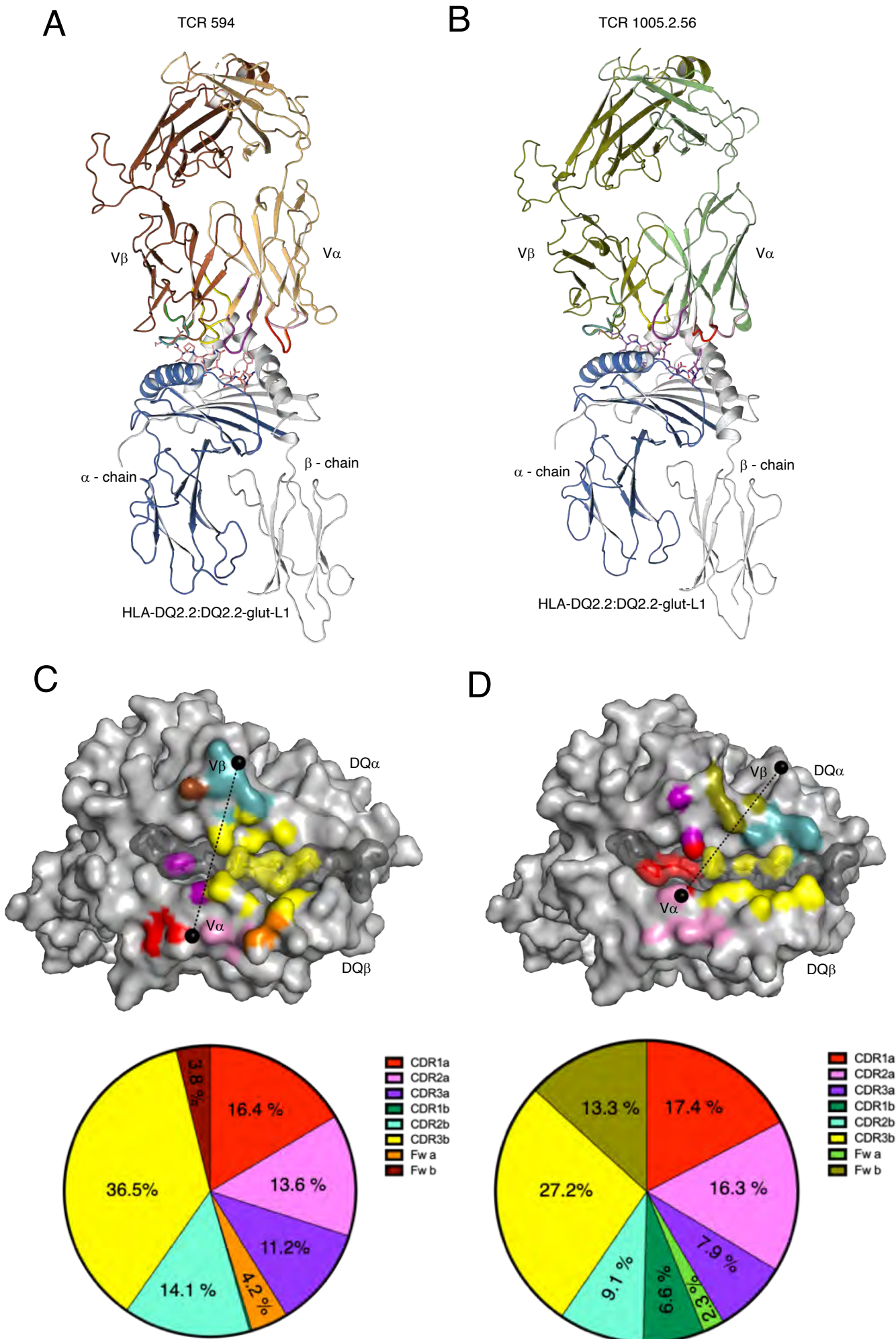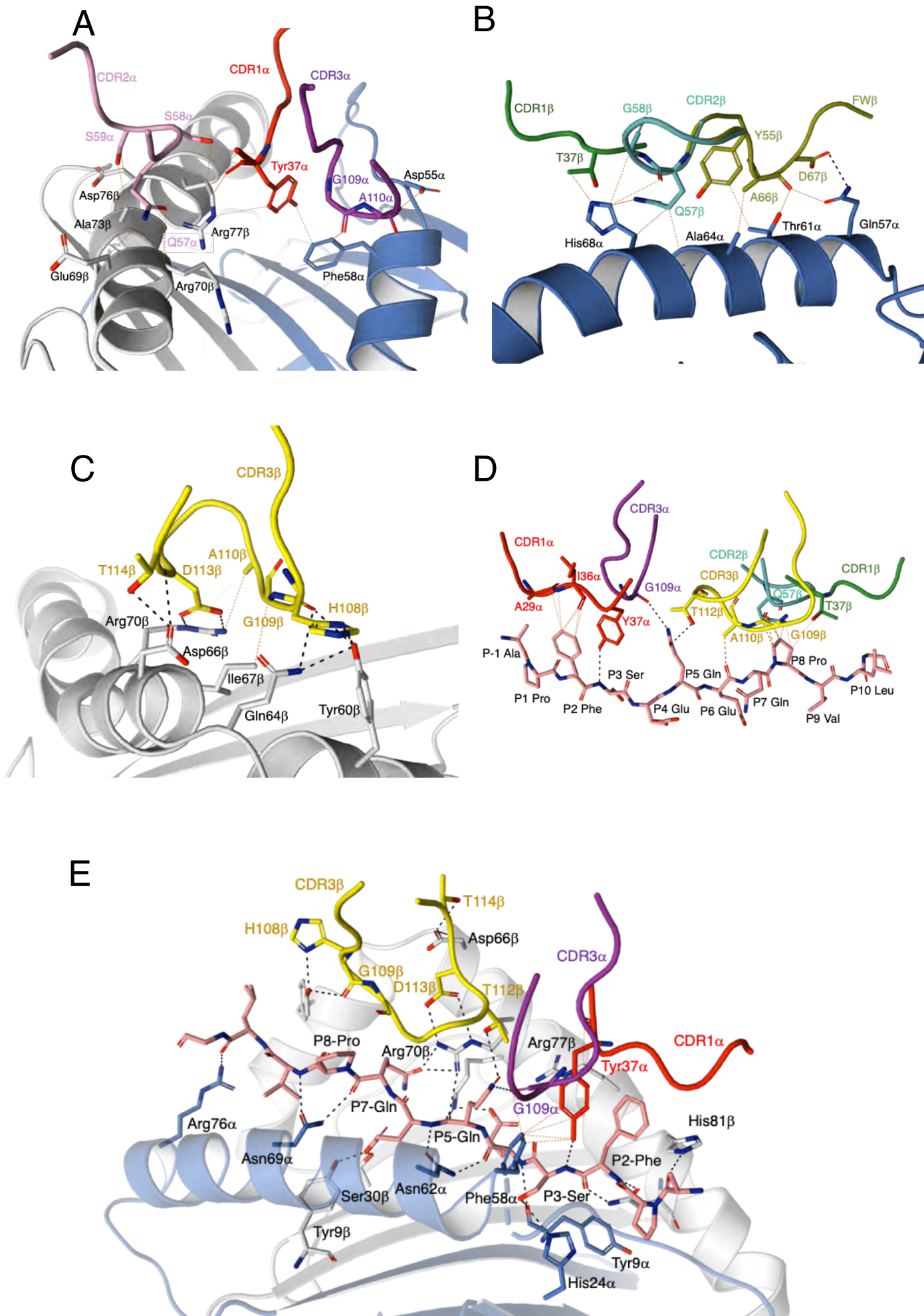
Figure 2.

Figure 3.

Figure 4.

Figure 5
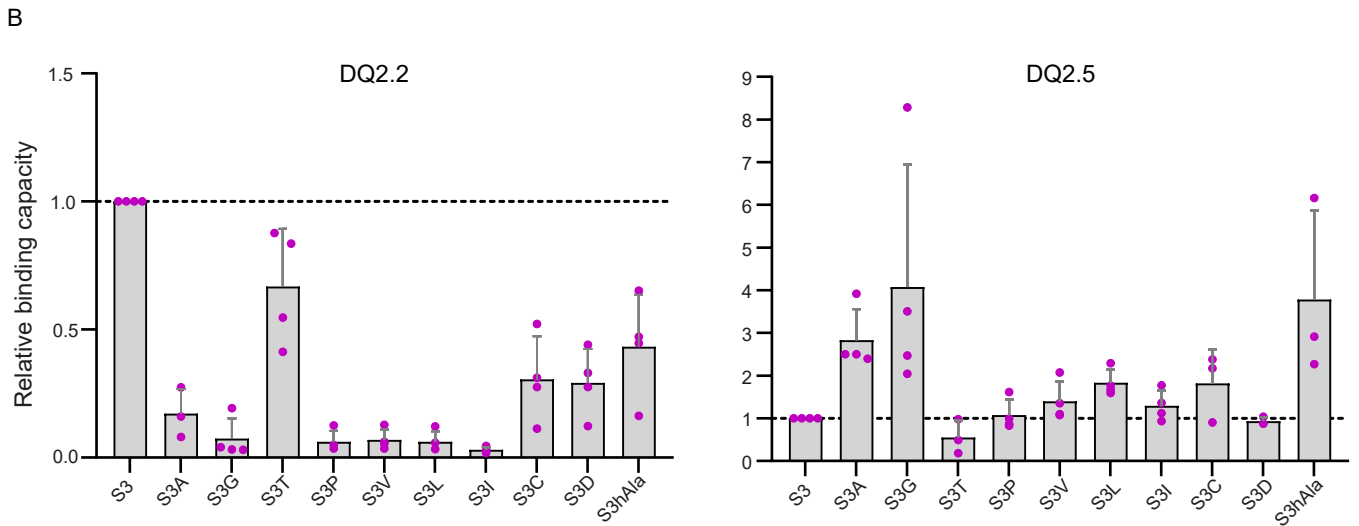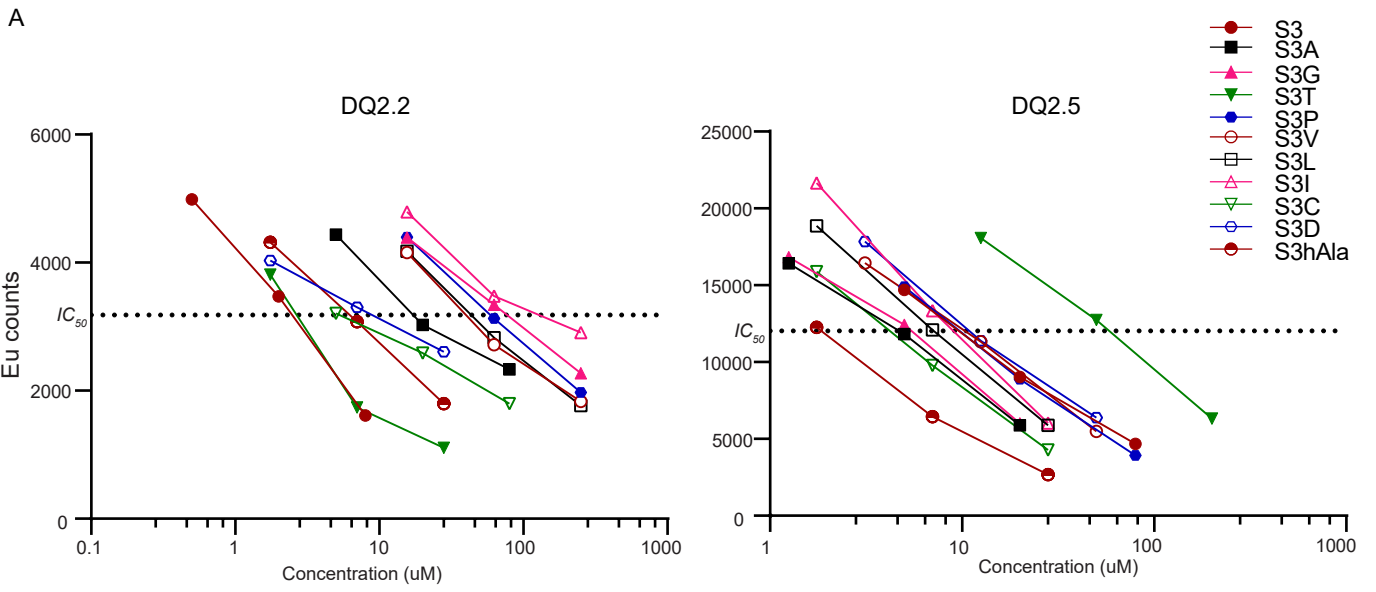
Figure 6.
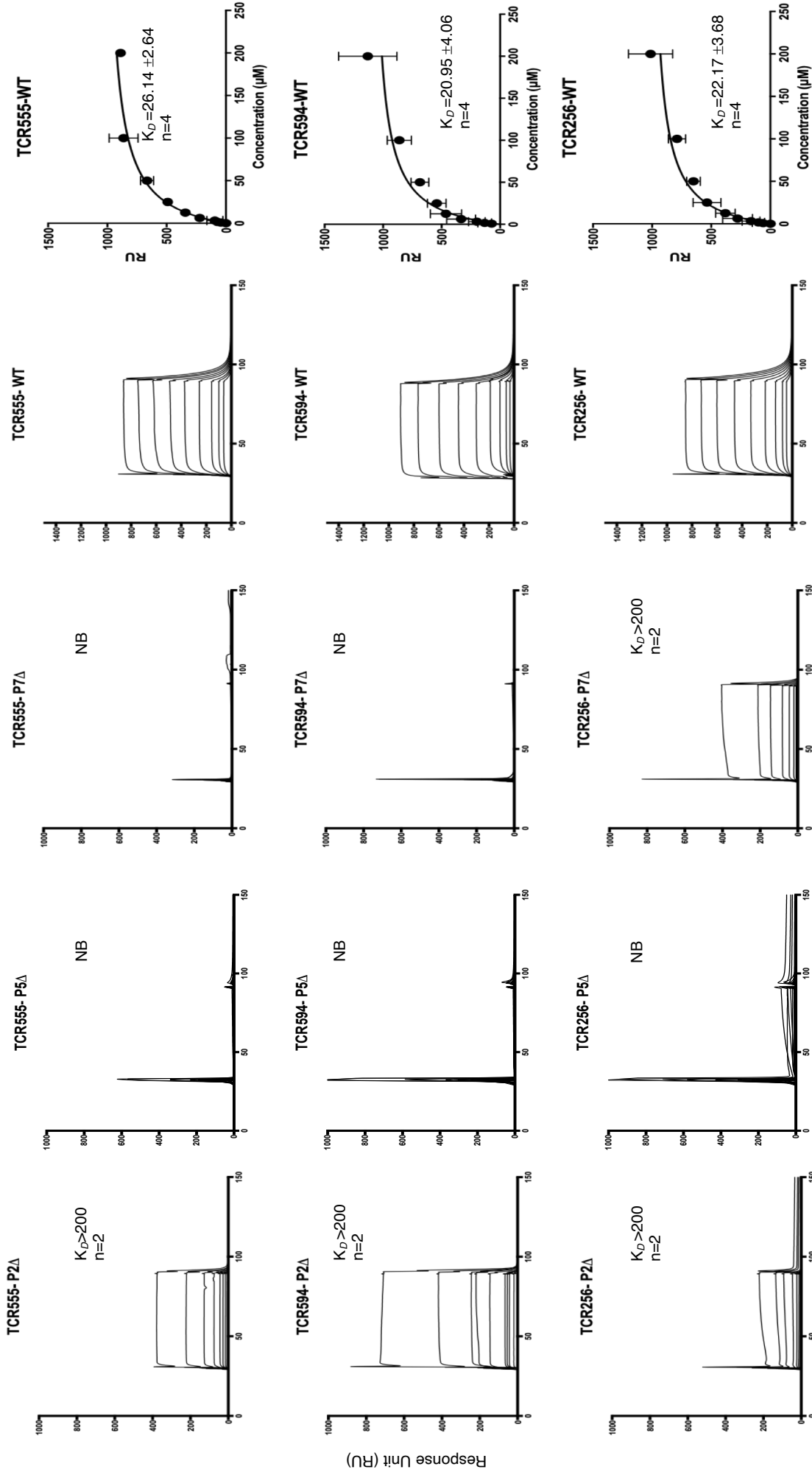
Table 1: DQ2.2-specific TCR sequences

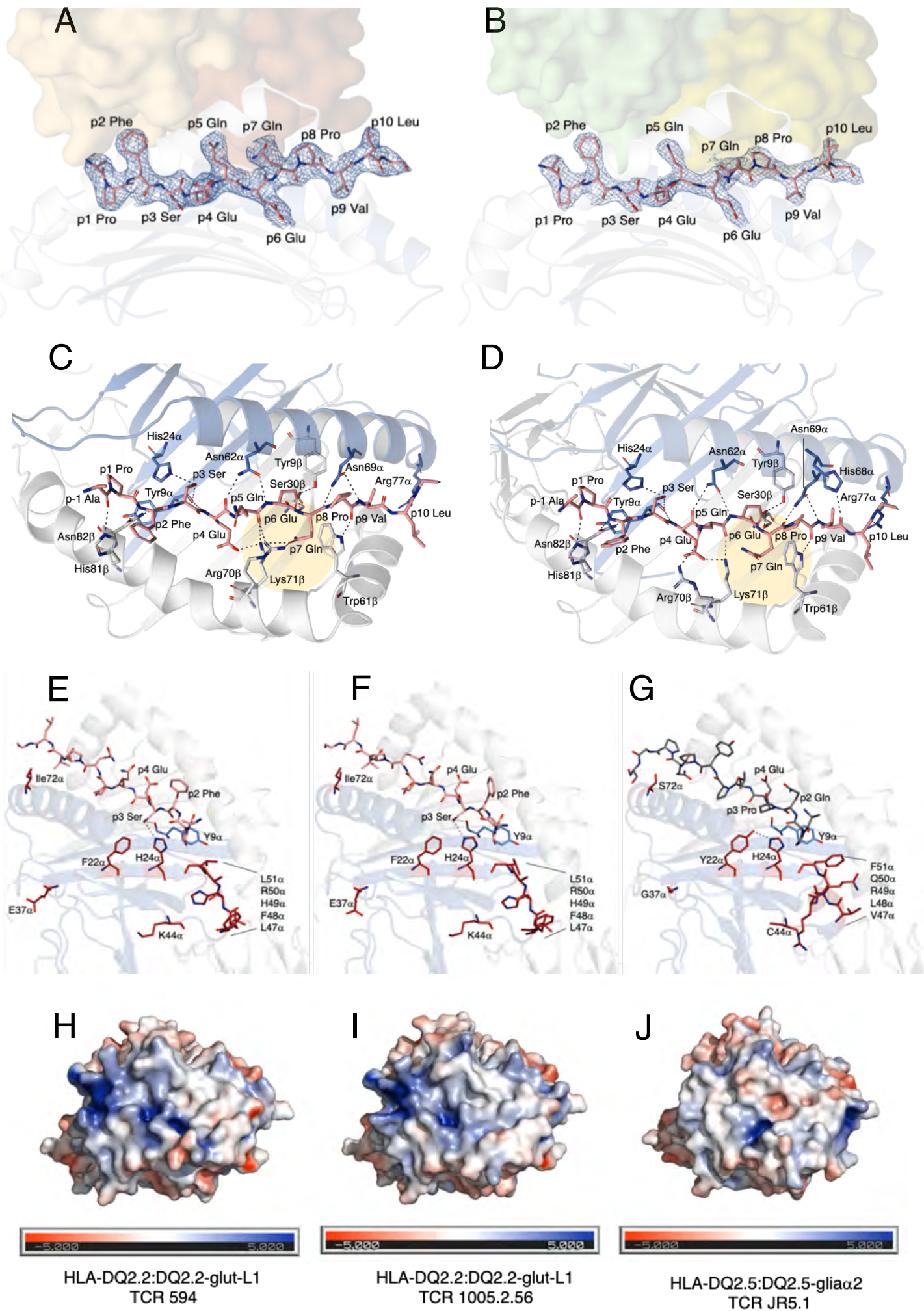| Nr	Donor	TRAV	TRAJ	CDR3a	TRBV	TRBD	TRBJ	CDR3b	Nr of cells	TCC
1	1005	12-3	34	CAMTLNTDKLIF	4-2	1	1-2	CASSLQGGDYGYTF	1	
2	1005	38-1*01	32*02	CAFMKEDGGATNKLIF	20-1*01	1*02	2-5*01	CSASPGNTGVAQYF	5	TCC1005.2.54 & TCC1005.2.60
3	1005	26-1	48	CIVYLSNFGNEKLTF	5-5	2	2-2	CASSLIGGGELFF	1	
4	1005	29/DV5	42	CAASAHYGGSQGNLIF	12-5	1	1-1	CASGPGTATEAFF	1	
5	1005	38-2/DV8	58	CAYRSQETSGSRLTF	20-1	1	2-5	CSASWLGFGETQYF	9	
6	1005	38-2/DV8	58	CAYTPLETSGSRLTF	20-1	1	2-7	CSARAPITGRFYEQYF	4	
7	1005	21	42	CAVRPGGSQGNLIF	4-2	2	2-5	CASSLTTSEETQYF	74	
		29/DV5	30	CAASADLTNRDDKIIF						
8	1005	38-1	42	CAFMKGSYGGSQGNLIF	7-8	1	2-7	CASSRTANYEQYF	28	
		40	40	FLLGITSGTYKYIF						
9	1005	26-1	54	CIVRVAEGAQKLVF	20-1		2-5	CSATKETQYF	1	
10	1005	26-1	54	CIVRVAEGAQKLVF	20-1	1	2-5	CSATKETQYF	3	
11	1005	21*02	31*01	CAVHTGARLMF	7-3*01	1*01	2-3*01	CASSHGASTDTQYF	NA	TCC1005.2.56, TCC1005.2.57, TCC1005.2.58, TCC1005.2.62 & TCC1005.2.65
12	555	26-1	54	CIVRVAEGAQKLVF	20-1		2-5	CSATKETQYF	3	
13	555	6	26	CALVRDYGQNFVF	7-2	2	2-7	CASSTSGGGARSYEQYF	1	
14	555	1-1*01	9*01	CAWTGGGGFKTIF	6-2*01	2*01	2-7*01	CASRKPGGDYEQYF	80	TCC555A.1.4.38
15	555	21	58	CAVIGTSGSRLTF	7-3	1	2-3	CASSSGAATDTQYF	166	
16	594	26-1	54	CIVRPAQGAQKLVF	29-1	2	1-2	CSVSSGGEGGNGYTF	1	
17	594	9-2*01	57*01	CASPQGGSEKLVF	11-2*01	1*01	1-1*01	CASSSGGWGGGTEAFF	62	TCC594.5.2.6**
		27	21	CAGRDDFNKFYF						
18	627	6	39	CALGLNNNAGNMLTF	10-3	1	2-5	CAISPRQAETQYF	1	
19	627	21	11	CAASGYSTLTF	11-1	1	2-3	CASTHGAGSDTQYF	108	
20	627	3*01	8*01	CAVSGNTGFQKLVF	28*01	2*02	1-5*01	CASTSRGGNSNQPQHF	NA	TCC627.1.3.199
		DV1*01	12*01	CALGATVMDSSYKLIF						

The table shows the total overview of unique TCRαβ paired sequences generated from high-throughput sequencing of HLA-DQ2.2:DQ2.2-glut-L1 tetramer-sorted single T cells and/or by Sanger sequencing of DQ2.2-glut-L1-specific TCCs. Due to uncertainty in the allele assignment in the TCRαβ sequences generated from single cell TCR sequencing approach, the alleles for the V, D and J genes are not shown for the TCRαβ sequences observed only in the single cell TCR sequencing data. Three TCRαβ sequences generated from single cell TCR sequencing (Nr. 2, 14 and 17) were also found to be expressed by the DQ2.2-glut-L1-specific TCCs, which are mentioned in rightmost column. Two of the TCRαβ sequences (Nr. 11 and 20) were observed only by Sanger sequencing of DQ2.2-glut-L1-specific TCCs (last column) and not observed in TCR sequencing data of HLA-DQ2.2:DQ2.2-glut-L1 tetramer sorted cells.

**: By performing Sanger sequencing we observed that TCC594.5.2.6 expresses single TCRα chain (TRAV9-2*01/TRAJ57*01). However, by performing single cell TCR sequencing, we were able to identify T cells that expressed an additional TCRα chain (TRAV27/TRAJ21).

Table S1. HLA-DQA1 and HLA-DQB1 alleles of CeD patients

CeD patient	Genotype[#]
627	*DQA1*02:01/03:02*
	*DQB1*02/03:03*
594	*DQA1*02/*
	*DQB1*02*
555	*DQA1*02:01/03:02*
	*DQB1*02/03:03*
1005	*DQA1*02:01/01:01*
	*DQB1*02:02/05:01*

Table S2. Data collection and refinement statistics

	Parameter	T594	T1005.2.56
Data Collection	Space Group	C 2 2 21	P 1 21 1
	Unit Cell Dimensions		
	a, b, c (Å)	75.28, 275.14, 141.55	72.534, 99.416, 72.565
	a, b, g (°)	90, 90, 90	90, 118.26, 90
	Resolution	45.86 – 2.83 (2.93-2.83)	39.24 - 3.0 (3.18 - 3.0)
	Data completeness (%)	85.0 (99.0)	99.9 (100)
	CC1/2	0.998 (0.854)	0.98 (0.667)
	Multiplicity	2.0 (2.0)	3.5 (3.5)
	Mean I/Sigma I	10.95 (1.90)	4.21 (1.50)
	R_{merge} (%)	3.36 (33.82)	10.26 (41.82)
	R_{meas}	4.76 (47.82)	14.52 (59.15)
	Total no. observations	71075 (6973)	35949 (3571)
	Total no. unique	35664 (462)	18263 (1814)
Refinement	R_{work}	0.2125	0.2050
	R_{free}	0.2517	0.2578
	RMS Bond lengths (Å)	0.004	0.003
	RMS Bond angles (°)	0.65	0.60
	Ramachandran favored (%)	93	93
	Ramachandran allowed (%)	7.2	6.7
	Ramachandran outliers (%)	0.25	0.13

Table S3. TCR594 TCR contact with HLA-DQ2.2

CDR loop	TCR residue		HLA residue		contact
CDR1α	Tyr30		Asp66β		vdw
			Asp76β		vdw
			Arg80β		vdw
			His81β		vdw
FWα	Lys55	NZ	Asp66β	OD1	H-bond
		NZ	Glu69β	OE1	H-bond
			Glu69β		vdw
CDR2α	Thr57		Glu69β		vdw
			Ala73β		vdw
	Lys58		Arg72β		vdw
CDR3α	Glu112	OE1, OE2	Arg70β	NH1, NH2	salt bridge
			Arg77β		vdw
CDR2β	Gln57		Phe58α		vdw
			Gln57α		vdw
			Thr61α		vdw
	Asn58		Thr61α		vdw
	Gly64		Lys39α		vdw
			Gln57α		vdw
FWβ	Val66		Asp55α		vdw
CDR3β	Trp111		Phe58α		vdw
			Thr61α		vdw
		NE1	Asn62α	OD1	H-bond
			Val65α		vdw
	Gly112		Phe58α		vdw
			Thr61α		vdw
			Ile67β		vdw
			Arg70β		vdw
			Arg77β		vdw
	Gly113		Asp66β		vdw
			Arg70β		vdw

	Gly114		Ile67β		vdw
	Thr115		Asp66β		vdw
			Arg70β		vdw
	Glu116	OE1	Asp66β	OD1	H-bond
		OE1	Asp66β	OD2	H-bond
			Arg70β		vdw

Table S4 TCR1005.2.56 contact with HLA-DQ2.2

CDR loop	TCR residue		HLA residue		contact
CDR1α	Tyr37		Phe58α		vdw
			Arg77β		vdw
CDR2α	Gln57		Glu69β		vdw
			Arg70β		vdw
			Ala73β		vdw
	Ser58		Arg77β		vdw
	Ser59		Ala73β		vdw
			Asp76β		vdw
CDR3α	Gly109		Phe58α		vdw
	Ala110		Asp55α		vdw
CDR1β	Thr37		His68α		vdw
CDR2β	Gln57		Ala64α		vdw
			Val65α		vdw
			His68α		vdw
	Gly58		His68α		vdw
CDR3β	His108	O	Tyr60β	OH	H-bond
		ND1	Tyr60β	OH	H-bond
		O	Gln64β	NE2	H-bond
	Gly109	N	Gln64β	OE1	H-bond
			Ile67β		vdw
	Ala110		Arg70β		vdw
	Thr112	OG1	Arg70β	NE	H-bond
	Asp113		Ile67β		vdw
		OD1	Arg70β	NE	H-bond
		OD2	Arg70β	NH2	H-bond
	Thr114	OG1	Asp66β	OD1	H-bond
		N	Asp66β	OD1	H-bond
FWβ	Tyr55		Thr61α		vdw
	Ala66		Gln57α		vdw
			Thr61α		vdw
			Ala64α		vdw
	Asp67		Gln57α		vdw
		OD1	Gln57α	NE2	H-bond

Table S5. TCR contact with DQ2.2-glut-L1 peptide

TCR594

CDR loop	TCR residue		Peptide residue		contact
CDR3α	Gly109		P2-Phe		vdw
	Gly110		P2-Phe		vdw
	Glu112		P2-Phe		vdw
CDR3β	Gly109	O	P5-Gln	NE2	H-bond
	Gly110	O	P5-Gln	NE2	H-bond
		O	P7-Gln	OE1	H-bond
		O	P7-Gln	NE2	H-bond
	Trp111		P5-Gln		vdw
			P6-Glu		vdw
			P7-Gln		vdw
			P8-Pro		vdw
	Gly112		P5-Gln		vdw
		N	P7-Gln	OE1	H-bond
			P8-Pro		vdw

TCR1005.2.56

CDR loop	TCR residue		Peptide residue		contact
CDR1α	Ala29		P2-Phe		vdw
	Ile36		P2-Phe		vdw
	Tyr37	OH	P3-Ser	N	H-bond
CDR3α	Gly109	O	P5-Gln	NE2	H-bond
CDR1β	Thr37		P8-Pro		vdw
CDR2β	Gln57		P8-Pro		vdw
CDR3β	Gly109		P8-Pro		vdw
	Ala110		P6-Glu		vdw
	Thr112	OG1	P5-Gln	OE1	H-bond

Table S6: Peptide variants of the DQ2.2-glut-L1 epitope analyzed in the competitive peptide binding assay

	Name	Sequence
1	S3	Ac-QQPPFSEQEQPVLPQ
2	S3A	Ac-QQPPF**A**EQEQPVLPQ
3	S3G	Ac-QQPPF**G**EQEQPVLPQ
4	S3T	Ac-QQPPF**T**EQEQPVLPQ
5	S3P	Ac-QQPPF**P**EQEQPVLPQ
6	S3V	Ac-QQPPF**V**EQEQPVLPQ
7	S3L	Ac-QQPPF**L**EQEQPVLPQ
8	S3I	Ac-QQPPF**I**EQEQPVLPQ
9	S3C	Ac-QQPPF**C**EQEQPVLPQ
10	S3D	Ac-QQPPF**D**EQEQPVLPQ
11	S3hAla	Ac-QQPPF(**AABA**)EQEQPVLPQ where (AABA): α-aminobutyric acid

The nine amino acid core sequence of DQ2.2-glut-L1 is underlined
Substituted amino acids are boldfaced